JOURNAL OF MATERIALS SCIENCE 21 (1986) 3777–3782

Hydrogen-induced cracking in two linepipe steels

K. K. CHAWLA*, J. M. RIGSBEE
Department of Metallurgy and Mining Engineering, University of Illinois at Urbana–Champaign, 1304 W. Green, Urbana, Illinois 61801, USA

J. B. WOODHOUSE
Materials Research Laboratory, University of Illinois at Urbana–Champaign, 104 S. Goodwin, Urbana, Illinois 61801, USA

Linepipe steels are susceptible to hydrogen-induced cracking (HIC) in wet, sour gas environments. Two commercially produced linepipe steels were investigated with regard to HIC on cathodic charging. Both steels, B and C, showed a high banded microstructure consisting of alternative layers of polygonal ferrite and a mixture of non-ferritic constituents (pearlite, bainite, and martensite–austenite). The degree of banding was higher in Steel B than in Steel C. Also present were elongated inclusions in Steel B, while in Steel C they were more or less equiaxed. On cathodically hydrogen-charging in the absence of external stress, microvoids formed at low current densities at or around inclusions. On prolonged charging, these voids grew and propagated parallel to the bands, running along the interface between ferrite/non-ferrite constituents, along inclusions lodged in the non-ferritic consitituents, and at places through the non-ferritic constituents. Steel B, not unexpectedly, showed more severe permanent microstructural damage than Steel C, leading to the conclusion that a high banded structure and/or the presence of elongated inclusions is deleterious to resistance against HIC.

1. Introduction

Hydrogen-induced cracking (HIC) can be a serious problem in linepipe steels when the transport of gas or oil containing H_2S is involved. HIC commonly occurs as blistering or stepwise cracking in low- and medium-carbon steels in the absence of an external stress [1–5]. Sulphide stress-corrosion cracking (SSCC) is more likely in high-strength steels under stress. Thus, SSCC in linepipe steels can be a problem in high hardness regions around weldments [1]. Both HIC and SSCC result from the entry of atomic hydrogen into steel and its precipitation as molecular hydrogen at inclusions or other microstructural sites. When the internal pressure exceeds a critical value, HIC ensues.

A wet, sour gas environment is a good source of atomic hydrogen generation. Manganese sulphide inclusions, elongated in the rolling direction, are perhaps the worst culprits in this regard. Additionally, the accentuated banded structure produced by the controlled rolling practice of very low-temperature finishing will be expected to play an important role in HIC of such steels. In this paper we report on the damage produced in two commercially obtained, controlled-rolled niobium–vanadium containing X-70 type steels on cathodically hydrogen-charging, and we relate this damage to the microstructural features.

2. Experimental procedure

The chemical composition of the two steels, designated B and C, is given in Table I. Samples 15 mm × 10 mm × 2.5 mm were cut from the steels and polished to 600 grit, followed by finishing on diamond wheels.

Metallographic samples from the two steels were polished and etched with picral and examined in an optical and a scanning electron microscope, JEOL JSM-35. A detailed analysis of the initial structure was also made by means of transmission electron microscopy (Philips EM430) and energy-dispersive X-ray microchemical analysis.

Cathodic hydrogen-charging was done at room temperature in an aqueous 1 N solution of H_2SO_4 saturated with As_2O_3 as the recombination poison. The current density used was 100 mA cm^{-2}, while the charging times varied from 1 to 24 h with an applied negative voltage of about 3.5 V. The samples (as-polished and after etching) were observed in a JEOL JSM-35 SEM coupled with an energy-dispersive analyser. Observations were also made of specimen cross-sections by polishing and etching the samples in 4% picral.

TABLE I Chemical composition of steels (wt %)

	C	Mn	P	S	Si	V	Nb
Steel B	0.08	1.57	0.017	0.003	0.26	0.08	0.03
Steel C	0.11	1.53	0.012	0.004	0.30	0.07	0.04

**Present address*: Department of Materials and Metallurgical Engineering, New Mexico Institute of Mining and Technology, Socorro, New Mexico 87801, USA.

0022–2461/86 $03.00 + .12

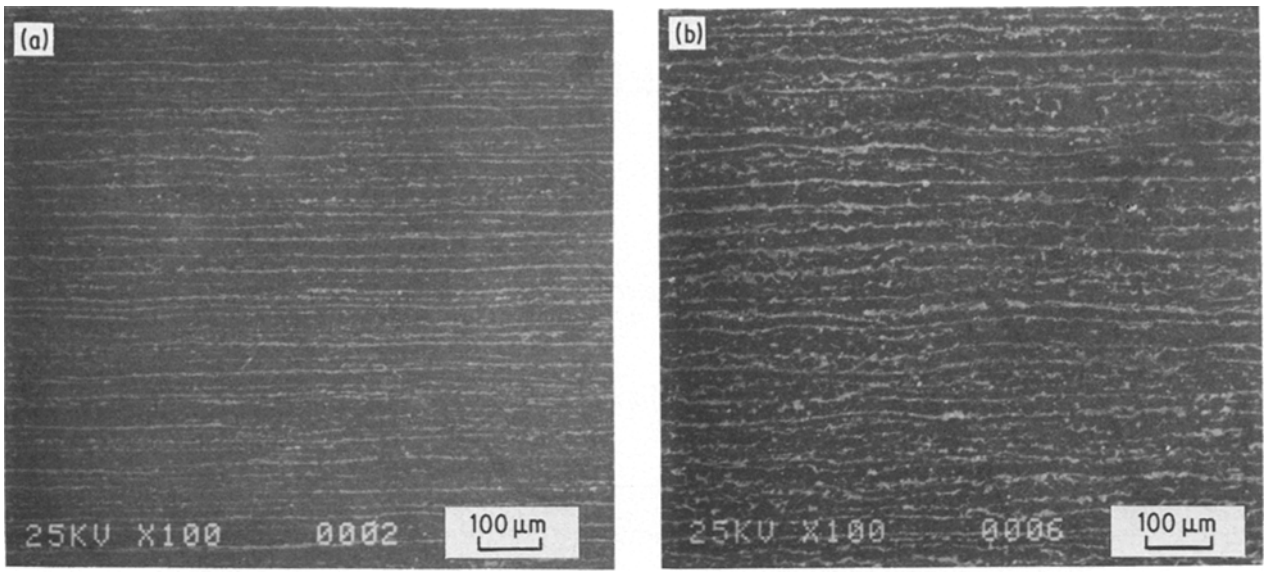

Figure 1 Banded microstructure of (a) Steel B, (b) Steel C. The degree of banding is higher in Steel B than in Steel C.

3. Results and discussion

A detailed description of the initial microstructure has been given elsewhere [6]. Both steels, B and C, showed a high banded microstructure consisting of alternate layers of polygonal ferrite and non-ferritic consitituents (pearlite, bainite and/or martensite–austenite). Fig. 1 shows the banded structure of the two steels. Notice that the degree of banding is higher in Steel B than in Steel C. Inclusions, equiaxed or elongated, in such severely rolled steels tend to lodge themselves in the non-ferritic bands, as shown for Steel C in Fig. 2. Many inclusions in Steel B consisted of elongated stringers of MnS (Fig. 3). It would appear that Steel B was neither calcium-treated to obtain a low sulphur content nor treated with rare-earth elements for inclusion shape control. The microstructure as observed in TEM at higher magnifications was essentially the same in the two steels. Fig. 4a and b show the pinning of dislocations by small niobium and vanadium carbonitrides in Steels B and C, respectively. Thus, the essential microstructural differences between the two steels were (i) a higher degree of banding in Steel B than in Steel C, and (ii) more elongated inclusions in Steel B than in Steel C.

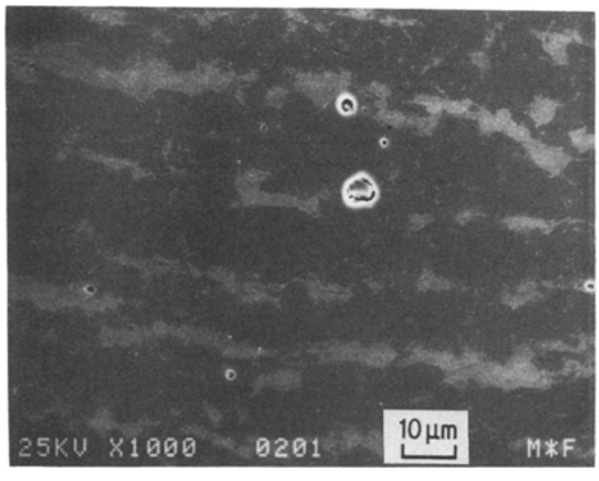

Figure 2 Inclusion (equiaxed) lodged preferentially in the non-ferritic band. Steel B. Etchant: picral.

It is well recognized that inclusions are one of the favoured types of site for microstructural damage due to hydrogen in such steels [1–3]. As pointed out above, the inclusions, whether elongated or not, tended to lodge in the non-ferritic band. This perhaps accentuated the effect of the banded structure. In any case, the initial effect of charging for low times was to produce damage consisting of voids at inclusions, generally located in or near the non-ferritic constituents. Fig. 5 shows this for Steel C charged for 1 h at 100 mA cm^{-2}. After 24 h of charging these microvoids, initiated at inclusions or at ferrite/non-ferritic interfaces, grew along the non-ferritic constituents or along the interface between ferrite and non-ferritic constituent, forming the so-called stepwise cracking. Fig. 6 shows this in an unetched condition. Notice the stepwise nature of cracking. Fig. 7 shows vividly the preferential alignment of these cracks along the non-ferritic band.

Steel B also showed initiation of voids at inclusions and/or at the non-ferritic constituent after a charging of 1 h at 100 mA cm^{-2} (Fig. 8). An aluminium-based inclusion lodged in a void in the same steel is shown together with Al$K\alpha$ mapping in Fig. 9. After 24 h of charging these voids grew into rather extensive stepwise cracks, as shown in the unetched condition in Figs. 10 and b. The cracks run parallel to the bands (not visible in this micrograph). Notice the greater amount of microstructural damage in Steel B (Fig. 10) than in Steel C (Fig. 6). The alignment of these hydrogen-induced cracks along the band existing in the structure is seen in Fig. 11, which shows the situation after etching.

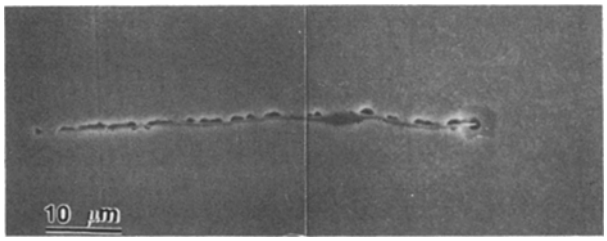

Figure 3 Elongated MnS inclusion in Steel B.

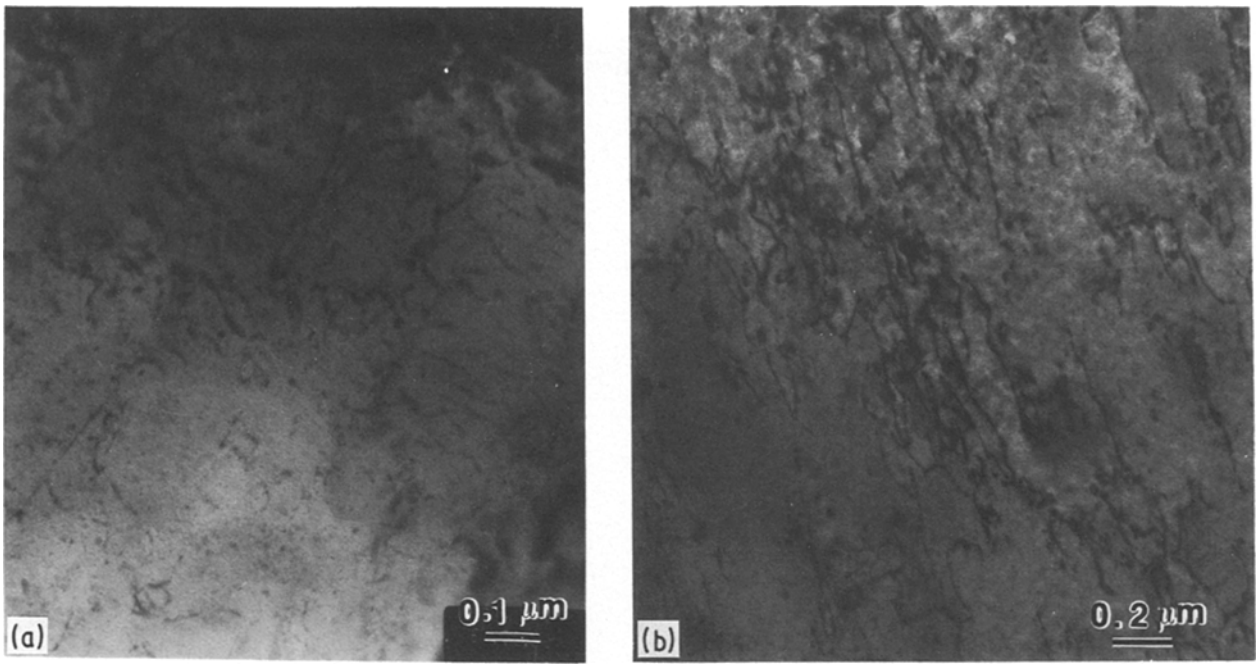

Figure 4 Dislocation pinning by fine carbonitrides of niobium and vanadium. (a) Steel B, (b) Steel C. TEM.

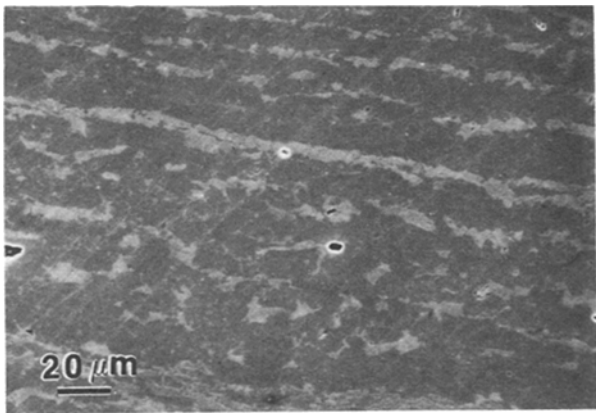

Figure 5 Microvoids at inclusions located in or near the non-ferritic band after 1 h charging. Steel C.

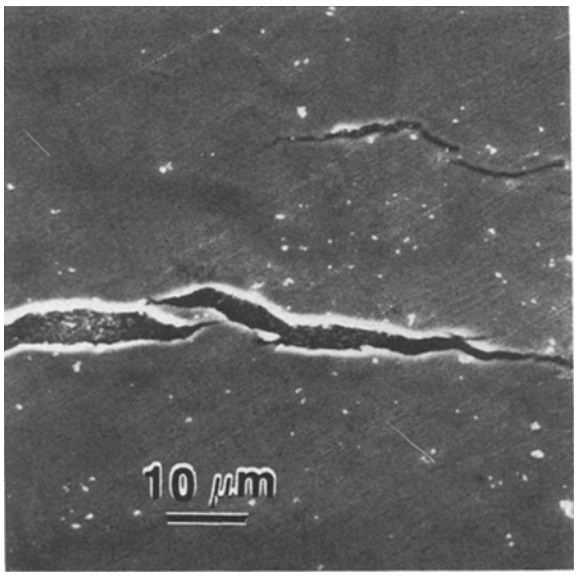

Figure 6 Stepwise cracking in Steel C after 24 h charging. Unetched.

In order to assess and compare the extent of microstructural damage in the two steels, we examined through-thickness sections. Fig. 12 shows that in Steel B after 24 h charging the damage extended completely through the thickness. This was not the case in Steel C. The preferential growth of cracks along the bands in Steel B is clearly seen in Fig. 13. Steel C, which showed a lesser degree of banding and less elongated inclusions than Steel B, suffered a markedly less through-thickness damage. The situation existing at about the mid-thickness position ($\sim$ 1 mm from the surface) after 24 h charging is shown in Fig. 14. In all

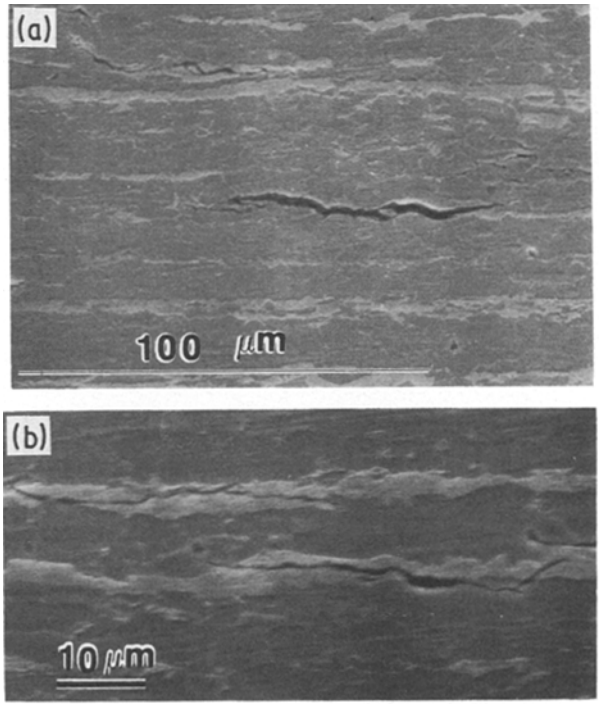

Figure 7 (a, b) Two different areas of Steel C, showing preferential alignment of cracks along the non-ferritic layers after 24 h charging. Etchant: picral.

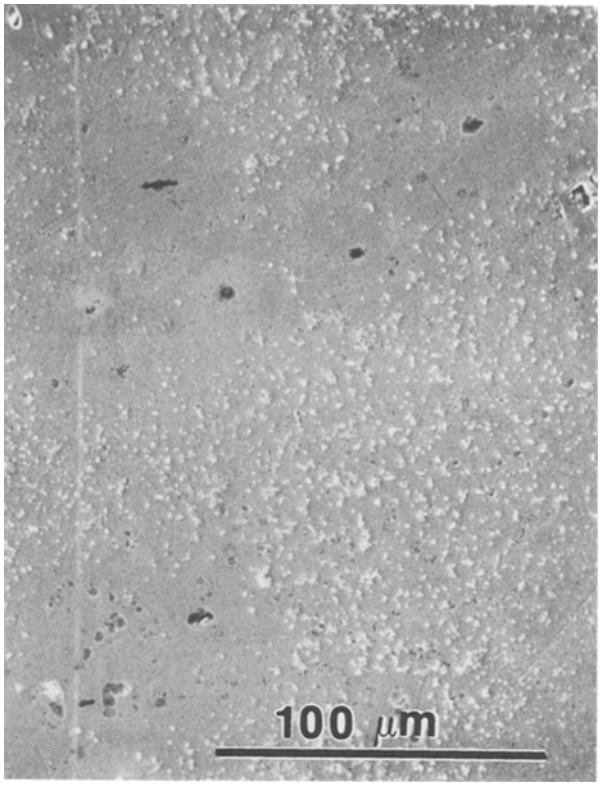

Figure 8 Microvoids at inclusions and/or at non-ferritic bands. 1 h charging. Steel B. Unetched.

probability, the void initiated at some inclusion and grew some distance along the band.

Hydrogen transport occurs by both diffusion through the lattice and along defects such as dislocations, grain boundaries and interphase boundaries. Atomic hydrogen diffuses in from the surface and recombines to precipitate as molecular hydrogen gas at inclusions at various preferred sites in the non-ferritic constituents. It should be recognized that non-lamellar pearlite, bainite, and martensite–austenite islands in the non-ferritic bands are essentially

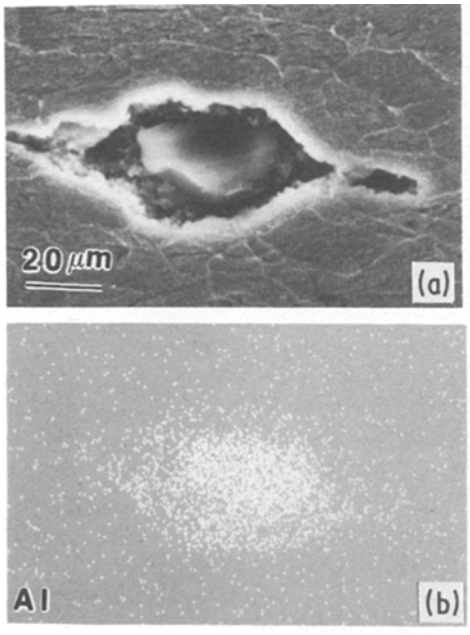

Figure 9 (a) An aluminium-based inclusion in the interior of a void; (b) Al$K\alpha$ mapping. Steel B, 1 h charging.

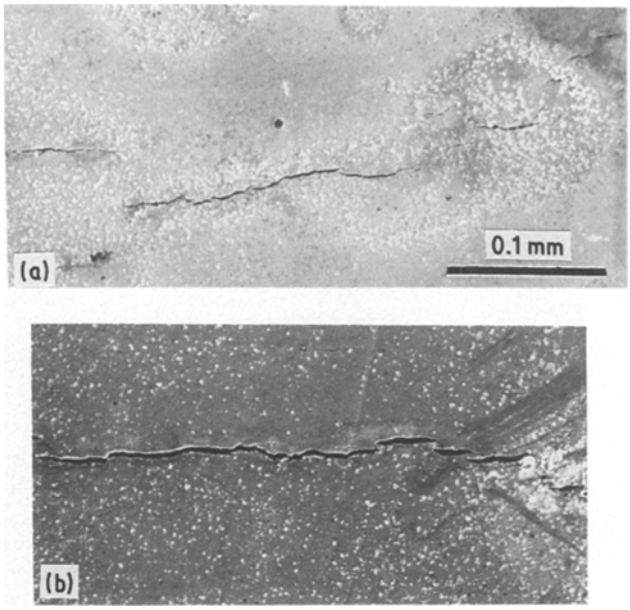

Figure 10 (a, b) Extensive stepwise cracking in Steel B after 24 h charging.

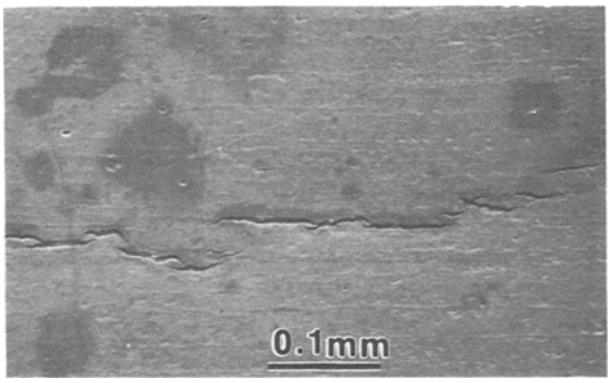

Figure 11 Alignment of cracks in steel with the bands in Steel B, seen after light etching with picral.

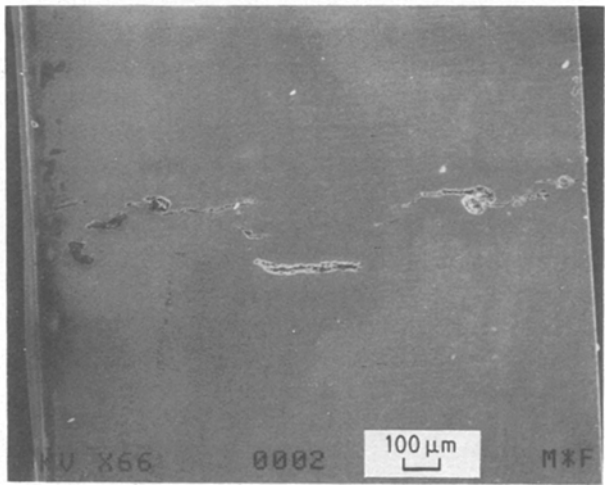

Figure 12 Through-thickness section of Steel B, showing damage due to HIC after 24 h charging.

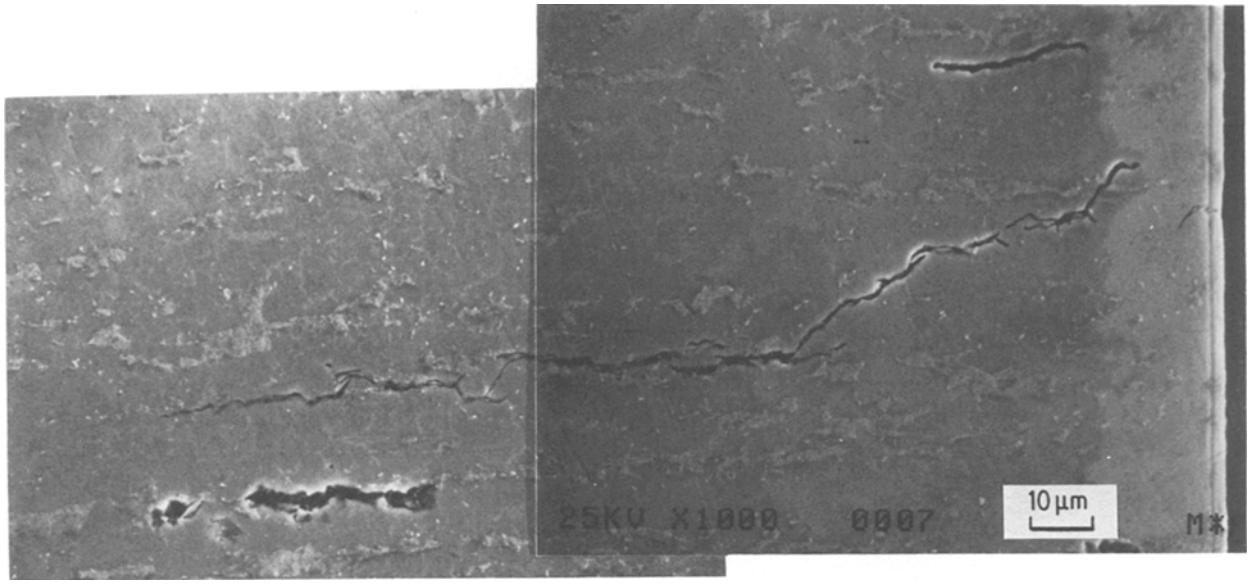

Figure 13 Alignment of cracks along the non-ferritic bands in the thickness direction of Steel B after 24 h charging.

inclusions, for void-initiation purposes. This precipitation of molecular hydrogen is known to generate pressure high enough to initiate void formation, and on continued charging it leads to the preferential growth of these voids along the pre-existing bands. In view of the fact that Steel B had a higher degree banding and more MnS-type stringers than Steel C, the appreciably larger amount of microstructural damage in the former is quite understandable. It is likely that the interface between ferritic/non-ferritic layers in these steels, much like an aligned grain boundary, provided a fast-transport medium for hydrogen and a distribution of sites for precipitation of H_2. Initially, the voids nucleated at ferrite matrix/inclusion or ferrite/pearlite (or bainite or martensite–austenite) interfaces near the surface. These voids grew into cracks parallel to the bands, along the elongated inclusions and through the non-ferritic constituents, and at times along ferrite/non-ferritic interfaces. Clearly, a more homogeneous microstructure with reduced banding would lead to a greater resistance against HIC.

The banded structure in these steels results from the segregation of manganese and the practice of low-temperature finishing [1, 5]. Thus, reducing the amount of manganese to a minimum, coupled with a high-temperature finishing, would yield steels more resistant to HIC. Low sulphur content and/or inclusion shape control would also be beneficial.

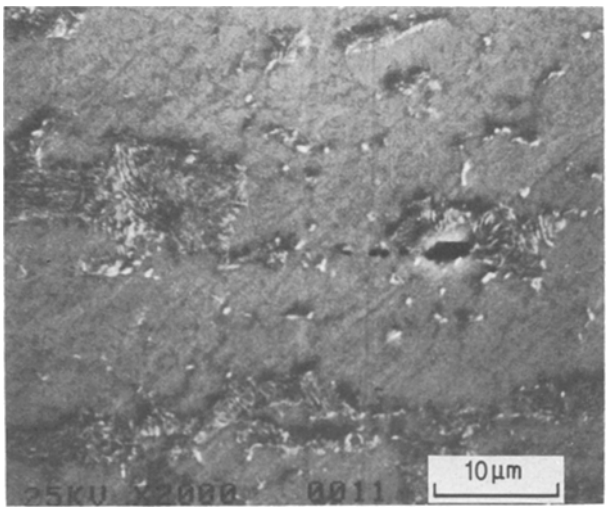

Figure 14 Damage in Steel C at about mid-thickness (~ 1 mm from the surface).

4. Conclusions

The higher degree of banding and the presence of more elongated inclusions in Steel B than in Steel C led to a greater incidence of HIC in the former under a given set of cathodic charging conditions. The ferrite matrix/inclusion interface, ferrite/non-ferritic constituents interface, and the aligned non-ferritic constituent itself, provided paths of easy crack growth on charging. An elimination of these characteristics (banded structure as well as elongated inclusions) via a lower manganese content and lower finish-rolling temperature, as well as an effective inclusion shape control, would improve resistance against HIC.

Acknowledgements

This work was supported in part by the Brazilian agencies CNPq, FINEP and Min. Ex. through the Materials Research Center of Instituto Militar de Engenharia. Partial support of this work by the Division of Materials Research of NSF under grant NSF-DMR-8303421 is gratefully acknowledged. Part of this work was done at the Center for Microanalysis of Materials in the Materials Research Laboratory of the University of Illinois, which is supported under contract DEACO2-176ER01198. K.K.C. acknowledges support from the Department of Metallurgy and Mining Engineering at the University of Illinois at Urbana–Champaign.

References

1. C. L. JONES, P. RODGERSON and A. BROWN, in "HSLA Steels: Technology and Applications" (ASM, Metals Park, Ohio, 1984) p. 809.
2. T. TAIRA and Y. KOBAYASHI, in "Steels For Linepipe and Pipeline Fittings" (The Metals Society, London, 1983) p. 170.

3. G. P. PRESSOUYRE, R. BLONDEAU and L. CADION, in "HSLA Steels: Technology and Applications" (ASM, Metals Park, Ohio, 1984) p. 827.
4. K. YAMADA, Y. SATOH, N. TANAKA, H. MURAYAMA, Z. CHANO and K. ITOH, in "HSLA Steels: Technology and Applications (ASM, Metals Park, Ohio, 1984) p. 835.
5. C. P. JU and J. M. RIGSBEE, *Mater. Sci. Eng.* **74** (1985) 47.
6. K. K. CHAWLA, J. M. RIGSBEE and C. R. MARIA, paper in preparation.

Received 25 July
and accepted 18 September 1985